Evaluation of optical propagation and radiation in optical waveguide using a numerical method

Mansour Bacha[1,2*] **and Abderrahmane Belghoraf**[2]

[1] *Space Technology Research Division, Centre of Satellites Development, BP 4065, Ibn Rochd USTO Oran, Algeria*

[2] *Electronics Department, University of Sciences and Technology of Oran Mohamed Boudiaf, BP 1505, Oran Elmnaouer, Algeria*

[*] *Corresponding author: bachamans@gmail.com*

Received February 6, 2014; accepted April 4, 2014; posted online June 20, 2014

We introduce a mathematical model based on a concept of intrinsic mode in order to analyse and synthesise optical wave propagation and radiation occurring in a non-uniform optical waveguide used in integrated optics as optical coupler. The model is based on numerical evaluation of electromagnetic wave by applying an intrinsic field integral to evaluate the field behaviour inside the optical waveguide. To analyse the field distribution inside the non-uniform waveguide and predict the beam propagation of optical energy involved in the propagation process, it is necessary to track the motion of any observation point along the tapered waveguide itself. Physically, the rays of the spectrum undergo reflections on the waveguide boundaries until the cut-off occurs and the phenomena of radiation begin. The numerical results show good agreement with those obtained by classical methods of evaluation used by other works.

OCIS codes: 080.1510, 130.3120, 230.7390.

doi: 10.3788/COL201412.070801.

An optical waveguide is a structure which guides the energy flow of an electromagnetic wave in a direction parallel to its interfaces[1,2]. The optical waves are transported by successive reflections at its interface. Typical dimensions of the optical waveguide are of the order of a micrometer and the energy in these waveguides can be coupled to the adjacent areas[2,3].

Though there are several types of optical couplers like the prism couplers the couplers by network, and grating coupler[4,5], the optical coupler with non-uniform thin film is distinguished by its simplicity and compatibility with planar technology circuits; it is thus used in several applications like detectors and mode converter[6,7].

The theoretical analysis of the non-uniform waveguides is much more difficult than that of the uniform waveguides; the difficulty is caused by its configuration which does not allow us the application of the method of separation of variables.

Several analytical and numerical methods have been applied to evaluate the optical propagation in optical waveguides[8−10], such as the beam propagation method (BPM)[11−13], the finite difference beam propagation method (FDBPM)[14] and effective index method[8,15], but these methods are much more complicated compared to the method introduced in this letter.

The basic structure of the non-uniform optical waveguide we study is illustrated in Fig. 1. The structure is constituted by a non-uniform waveguide layer of refractive indices (n_1) surrounded by a substrate of refractive indices (n_2) and an air-cover layer of refractive indices (n_3). The refractive indices values are defined as: $n_1 > n_2 > n_3$. The thickness T of waveguide decreases linearly, when the light is guided in the medium n_1 by successive reflections on waveguide boundaries.

A discrete number of rays emanating from the source X_0 reach the point X. Each beam can be characterized by the number of times it hits the B_{12} and B_{31} interfaces.

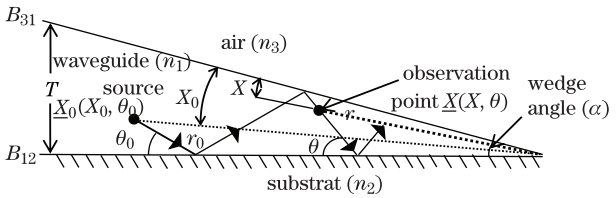

Fig. 1. Configuration of the non-uniform optical waveguide structure ($n_3 < n_2 < n_1$).

To analyse and predict the electromagnetic field distribution inside the optical waveguide as well as in the guided and leaky wave region, we have to track the motion of any observation point $\underline{X}$ along the non-uniform waveguide[6].

An incident ray in the non-uniform optical waveguide undergoes multiple reflections on the B_{12} interface (between the mediums n_1 and n_2) and B_{31} interface (between mediums n_1 and n_3). The angle of incidence increases gradually with decreasing thickness of the waveguide, so that the angle of incidence θ will exceed the critical angle characterizing the structure. The rays reaching an observation point 'X' after undergoing partial reflections will have small amplitudes compared to those who undergo total reflections on their course until reaching the point X.

After each pair of reflections on both interfaces B_{12} and B_{31}, the angle of incidence on B_{12} increases by adding twice the angle 'α' formed by the two interfaces B_{12} and B_{31}. This means that if we have m pairs of reflections on B_{12} and B_{31}, the new angle of incidence will become $(\theta + 2m\alpha)$[6,10]; α is very low. Consequently, at a certain point, the angle of incidence will become larger than the critical angle θ_c, and the energy will thus start to be refracted in the adjacent medium n_2. This energy will increase with the arrival of the subsequent light rays to form a beam of light emerging in the adjacent medium. Because of the refraction of the energy of non-uniform op-

tical waveguide to the adjacent medium (n_2), the waveguide is considered as an optical coupler in addition to its guiding property[16,17].

The relationship between the propagation constant β and the angle of incidence θ is

$$\beta = n_1 k_0 \cos(\theta). \tag{1}$$

In the guided region the following condition must be satisfied:

$$n_2 < \frac{\beta}{k_0} < n_1, \tag{2}$$

where β/k_0 is the effective index, $\beta/k_0 = n_2$ is the critical condition corresponding to the critical angle $\theta_c = \cos^{-1}(n_2/n_1)$. For $\beta/k_0 \leqslant n_2$ the field is cut off and becomes the radiation mode[6,8,9].

To analyse the electromagnetic field distribution inside the guide, and also to be able to predict the performances of our structure as encountered in integrated optics, the concept of an intrinsic integral $I(X,\theta)$ is introduced as[6,8,9]

$$I(X,\theta) = \frac{1}{\sqrt{2\alpha}} \int_C \exp[\mathrm{j}kS(X,\theta)]\mathrm{d}\theta. \tag{3}$$

The integral $I(X,\theta)$, which is a spectral integral, can be applied to any structure which has the wave propagation governed by the phase function $S(X,\theta)$ which will be presented later. Physically $I(X,\theta)$ describes a local mode generated by integrations over any angular plane waves spectrum. Such a source-free mode (labelled q) is defined at an observation point (X,θ) and propagates smoothly along the tapered waveguide with a wave number k.

The angle θ remains the angle of incidence of plane wave with respect to bottom boundary of the taper waveguide. The phase function $S(X,\theta)$ could be any phase among the four species of rays involved in the propagation process; they are fully developed in Ref. [10] and will be given below.

S_e^u and S_o^u represent the phases of waves which first go towards the upper interface (B_{31}) and have hit the B_{31} and B_{12} interfaces even or odd times respectively. S_e^d and S_o^d represent the phases of waves which first go towards lower interface (B_{12}) and have hit the B_{12} and B_{31} interfaces even or odd times respectively.

$$kS_e^u(\theta,\theta_0) = kS_c(\theta,\theta_0) + \frac{1}{2}\phi(\theta) + kr_0\cos(\theta_0 - \alpha - X_0) - kr\cos(\theta + \alpha - X), \tag{4}$$

$$kS_o^u(\theta,\theta_0) = kS_c(\theta,\theta_0) - \frac{1}{2}\phi(\theta) + kr_0\cos(\theta_0 - \alpha - X_0) - kr\cos(\theta - \alpha + X), \tag{5}$$

$$kS_e^d(\theta,\theta_0) = kS_c(\theta,\theta_0) + \frac{1}{2}\phi(\theta) + kr_0\cos(\theta_0 - \alpha + X_0) - kr\cos(\theta + \alpha + X), \tag{6}$$

$$kS_o^u(\theta,\theta_0) = kS_c(\theta,\theta_0) + \frac{1}{2}\phi(\theta) + kr_0\cos(\theta_0 - \alpha + X_0) - kr\cos(\theta + \alpha - X) - \pi, \tag{7}$$

$$kS_c(\theta,\theta_0) = \frac{1}{2}\phi(\theta_0) - \frac{1}{2a}\int_{\theta_c}^{\theta_0}\phi(\theta')\mathrm{d}\theta' + \frac{1}{2a}\int_{\theta_c}^{\theta}\phi(\theta')\mathrm{d}\theta' + \pi(1-2q)\frac{(\theta-\theta_0)}{2\alpha} + \pi(1-2q), \tag{8}$$

where $\phi(\theta)$ is the phase of the Fresnell reflection coefficient which can be expiessed as

$$\phi(\theta) = 2\arctan\mathrm{j}\sqrt{\frac{n_2^2 - n_1^2\cos^2(\theta)}{n_1^2 - n_1^2\cos^2(\theta)}}. \tag{9}$$

The zeroes of the derivative of the phase function ($kS_{eo}^{ud}(\theta,\theta_0)$) correspond to a characteristic equation or eigenvalues equation as[10]

$$\frac{\mathrm{d}S}{\mathrm{d}\theta}(X,\theta) = 0. \tag{10}$$

As an application numerical example, we will apply the method introduced in this letter to track the electromagnetic propagation optical wave along a non-uniform optical waveguide composed by a non-uniform waveguide layer of refracted indices $n_1 = 3.44$, substrate of refractive indices $n_2 = 3.36$, and the air cover layer of refractive indices $n_3 = 1$ at wavelength $\lambda = 1.55$ μm.

Using Newton Raphson method we find the corresponding solutions of the characteristic Eq. (10) which is developed in more details in Refs. [6,9]. It is illustrated in Fig. 2 which represents the variation of the effective index versus the non-uniform waveguide thickness. Figure 3 shows the cut-off thickness of the taper optical waveguide for the modes $1 \leqslant q \leqslant 10$; the cut-off thickness for each mode corresponds to β/k_0=3.36 in Fig. 2.

The energy starts to radiate to adjacent medium especially to medium (n_2) when the incident ray is very close and greater than the critical angle. For waveguide thickness less than cut-off thickness the angle of incidence becomes greater than the critical angle which causes the phenomena of optical radiation in the adjacent mediums (n_1 and n_2)[11].

In the guided wave region, all incident rays have an angle of incidence θ less than the critical angle θ_c. In the

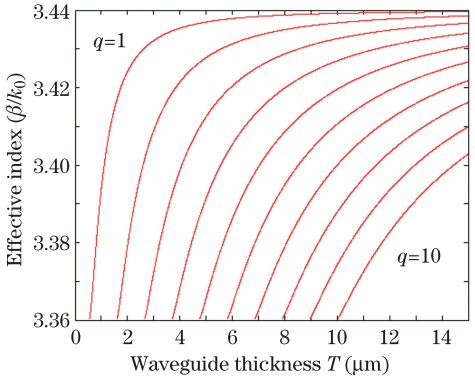

Fig. 2. Variation of the effective index versus waveguide thickness for the non-uniform optical waveguide ($n_1 = 3.44$, $n_2 = 3.36$, $n_3 = 1$ at λ=1.55 μm) for the modes: $1 \leqslant q \leqslant 10$.

radiation region the angle of incidence is limited by: $\theta_c < \theta < \pi/2$. Physically, the rays having the angle of incidence θ higher than $\pi/2$ have no mathematical contribution in intrinsic integral, i.e. Eq. (3). For this reason we evaluate the integral Eq. (3) in a contour of integration C limited by: $0< \theta < \pi/2$ using Simpson method[6,8].

In Figs. 4−6, electric fields are given as normalised fields to a maximum value of electromagnetic field for corresponding waveguide thickness. We notice in Fig. 4 that the normalised electric field of the first mode ($q = 1$) increases as the waveguide thickness decreases until it reaches the maximum value at T=0.794 μm, and it begins to diminish slowly until the cut-off thickness T_{c1}=0.535 μm. The intensity of the field decreases rapidly for thickness lower than the cut–off thickness.

We also notice in Figs. 5 and 6 that for the second mode (q=2) and the third mode (q=3), the normalised electric field increases as the waveguide thickness decreases until it reaches a maximum value and it begins to decrease rapidly after the cut-off thicknesses T_{c2}=1.586 and T_{c3}=2.638 corresponding respectively to the second and third modes.

We see in Fig. 6 that the maximum value of the normalised electric field intensity coincides with the normalised field intensity at the cut-off thickness. This is the case for all superiors modes (q >2).

We also notice that as the thickness decreases the electric field is pushed to adjacent mediums especially

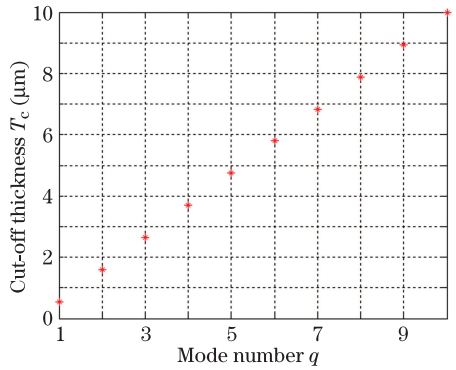

Fig. 3. Cut-off thickness for the non-uniform optical waveguide (n_1 = 3.44, n_2=3.36, n_3=1 at λ=1.55 μm) for the modes: 1⩽ q ⩽10.

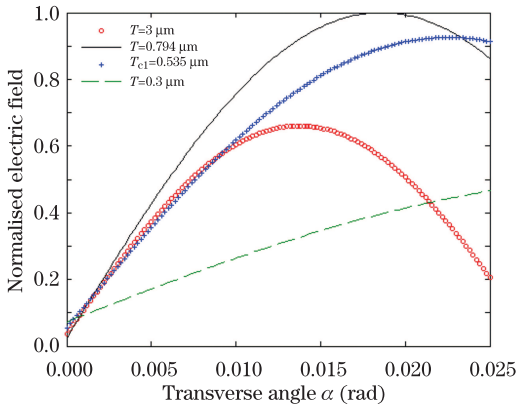

Fig. 4. Normalised electric field intensity inside the non-uniform optical waveguide for thickness greater and lower than cut-off thickness T_{c1}=0.535 μm for the first mode q=1.

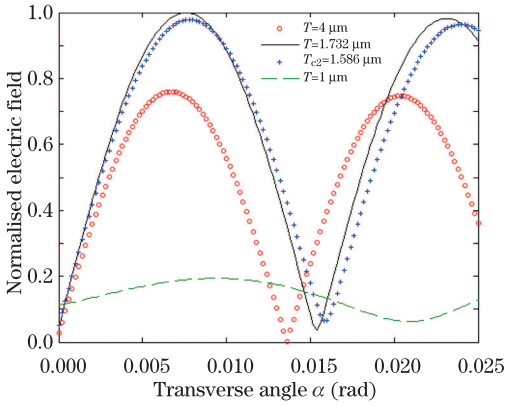

Fig. 5. Normalised electric field intensity inside the non-uniform optical waveguide for thickness greater and lower than cut-off thickness T_{c2}=1.586 μm for the second mode $q = 2$.

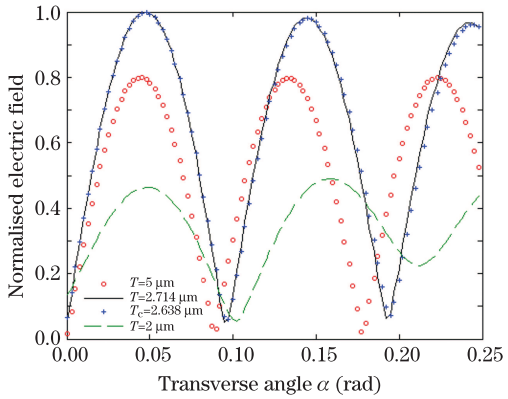

Fig. 6. Normalised electric field intensity inside the non-uniform optical waveguide for thickness greater and lower than cut-off thickness T_{c3}=2.638 μm for the third mode $q = 3$.

to substrate (n_2) corresponding to transverse angle α greater than 0.025 rds. After the cut-off thickness the maximum energy is present in the medium n_2, corresponding to the phenomena of radiation; an optical beam emerges from the waveguide film n_1 and is coupled to the substrate (n_2). The phenomena of radiation are predicted by the geometrical optics theory and from experimental work[9,18].

The simulation results concords with those obtained using other methods such as BPM and FDBPM[13−15].

In conclusion, by using an intrinsic integral we systematically evaluate the electromagnetic field distribution inside the non-uniform optical waveguide known as taper optical waveguide. The implementation of the intrinsic integral as a numerical computational tool gives results in excellent agreement with those in other references using different techniques. Before cut-off, results show that the electromagnetic field is concentrated in non-uniform optical waveguide corresponding to medium n_1 whereas when the angle of incidence becomes greater than critical angle the energy is radiated rapidly in the substrate medium (n_2). Moreover, for the universality of intrinsic concept, we can apply the model to evaluate the electromagnetic field behaviour outside the waveguide (n_1) and determine the distribution of the field in the adjacent mediums (n_2) and (n_3), corresponding to the

phenomena of radiation and optical coupling; This will be demonstrated in future work.

This work was co-supported by the University of Sciences and Technology of Oran Mohamed Boudiaf (USTOMB) and the Centre of Satellites Development (CDS), Oran, Algeria.

References

1. K. Okamoto, *Fundamentals of Optical Waveguides* (Elsevier, Burlington, 2006).
2. A. Boudrioua, *Photonic Waveguides Theory and Applications* (ISTE, London, 2009).
3. G. Lifante, *Integrated Photonics: Fundamentals* (John Willey & Sons, Chichester, 2003).
4. W. Ling, Z. Sheng, C. Qiu, H. Li, A. Wu, X. Wang, S. Zou, and F. Gan, Chin. Opt. Lett. **11,** 041301 (2013).
5. A. J. Whang, S. Chao, C. Chou, C. Lin, C. Chang, K. Jhan, and C. Wang, Chin. Opt. Lett. **11,** 122201 (2013).
6. A. Belghoraf, AMSE J. Mod. Meas. Control General Phys. **74,** 51 (2001).
7. R. G. Hunsperger, *Integrated Optics: Theory and Technology* (Springer, New York, 2009).
8. J. M. Arnold, A. Belghoraf, and A. Dendane, IEE Proceedings J. **132,** 314 (1985).
9. A. Dendane and J. M. Arnold, IEEE J. Quantum Electron. **QE-22,** 1551 (1986).
10. M. Bacha and A. Belghoraf, Int. Rev. Mod. Sim. **6,** 1624 (2013).
11. V. Prajzler, H. Tuma, J. Spirkova, and V. Jerabek, Radioengineering. **22**, 233 (2013).
12. K. Kawano and T. Kitoh, *Introduction to Optical Waveguide Analysis* (John Willey & Sons, New York, 2001).
13. G. L. Yip, Integ. Opt. Cir. SPIE. **1583,** 240 (1991).
14. Y. T. Han, J. U. Shin, D. J. Kim, S. H. Park, Y. J. Park, and H. K. Sung, ETRI J. **25,** 535 (2003).
15. M. M. Ismail and M. N. Shah Zainuddin, Appl. Mech. Mater. **52-54,** 2133 (2011).
16. L. Virot, L. Vivien, J. Fédéli, Y. Bogumilowicz, J. Hartmann, F. Bœuf, P. Crozat, D. Marris-Morini, and E. Cassan, Photon. Res. **1,** 140 (2013).
17. R. Tao, X. Wang, H. Xiao, P. Zhou, and L. Si, Photon. Res. **1,** 186 (2013).
18. P. K. Tien, G. Smolinsky, and R. J. Martin, IEEE Trans. Microwave Theory Tech. **MTT-23,** 79 (1975).